

Efficient exciton dissociation via two-step photoexcitation in polymeric semiconductors

Carlos Silva, Anoop S. Dhoot, David M. Russell, Mark A. Stevens, Ana C. Arias, J. Devin MacKenzie, Neil C. Greenham, and Richard H. Friend

Cavendish Laboratory, University of Cambridge, Madingley Road, Cambridge CB3 0HE, United Kingdom

Sepas Setayesh and Klaus Müllen

Max-Planck-Institute for Polymer Research, Ackermannweg 10, D-55128, Mainz, Germany

(Received 30 January 2001; revised manuscript received 14 June 2001; published 11 September 2001)

We report that exciton dissociation occurs within 150 fs during ultrafast photoexcitation at moderately high fluence, with $\sim 10\%$ quantum efficiency, in a model electroluminescent π -conjugated polymer. This is apparently inconsistent with the otherwise well-supported view that spin-singlet electron-hole pairs (excitons) are the primary photoexcitations. However, we demonstrate that resonant sequential transitions account quantitatively for the photoinduced polaron-pair yield, with the lowest ($1B_u$) exciton as an intermediate. Efficient exciton dissociation occurs either from the resulting high-energy, even-parity (A_g) states, or during ultrafast thermalization. The yield of photoinduced polarons, on the other hand, is $<0.1\%$ under continuous-wave excitation, where access to high-energy states by sequential excitation is not significant.

DOI: 10.1103/PhysRevB.64.125211

PACS number(s): 71.35.Cc, 78.55.Kz, 78.47.+p

I. INTRODUCTION

Electroluminescent π -conjugated polymers have been the focus of intensive research since the report that light-emitting diodes (LEDs) can be fabricated with these materials.¹ Here we show that in clean, well-ordered polymeric semiconductors, charged excitations are produced within 150 fs during high intensity, ultrafast photoexcitation, with $\sim 10\%$ quantum efficiency. This is apparently inconsistent with the otherwise well-supported view that Coulombically bound, spin-singlet electron-hole pairs (excitons) are the primary photoexcitations as is required to explain the high electroluminescence quantum efficiency in LEDs.² However, we demonstrate that this high exciton dissociation yield results from successive photoexcitation, first to the lowest exciton, then to a higher-energy exciton that readily dissociates to polaron pairs. Our results indicate that direct dissociation of the lowest excited state is not a significant process in this class of materials.

The prospect of organic laser diodes³ renders the fundamental understanding of the nature of high-energy excited states in these semiconductors important. A previous report by Köhler *et al.* of the photovoltaic action spectrum for related materials demonstrated that in a certain class of high-energy excitonic states in conjugated polymers, relatively facile electron-hole separation is achieved by virtue of the delocalized nature of the excited-state wave function, but low excitonic states have sufficient binding energy to be overcome before dissociation is achieved.⁴ On the other hand, recent reports by Moses *et al.* have produced evidence for ultrafast charge generation in conjugated polymer films with 10% quantum efficiency.^{5,6} In that experiment, the $\pi \rightarrow \pi^*$ transition of the polymer was induced with femtosecond optical pulses, and infrared-active vibrational (IRAV) modes,⁷ which are signatures of charged excitations, were probed with variably delayed infrared femtosecond pulses. The dynamics of these were found to be uncorrelated with the singlet exciton dynamics. Furthermore, the ultrafast

charge generation yield was reported to be weakly dependent on excitation photon energy, such that the enhanced photocurrent at high photon energy reported by Köhler *et al.* was attributed to enhanced carrier mobilities as a result of excess photon energy. This led to the conclusion that photocarriers are produced directly, and are not generated from a secondary process (such as exciton bimolecular annihilation⁸), and was rationalized within a semiconductor band model.

Recent photocurrent cross-correlation measurements by Zenz *et al.*,⁹ and also performed independently by Müller *et al.*,¹⁰ provide clear indication that in semiconductor conjugated polymers, excited states accessed by sequential excitation produce charge photocarriers, with the first excited singlet state as an intermediate. In these experiments, a femtosecond pulse resonant with the $\pi \rightarrow \pi^*$ gap excites the polymer, sandwiched between electrodes in a photovoltaic diode configuration. The change in photocurrent when a second femtosecond pulse is transmitted through the device is then recorded as a function of delay between the two pulses. Both papers conclude that the state accessed by sequential transitions has a higher dissociation probability than the first singlet excited state. We note that in these studies, excited states that lie 1.59 (Ref. 9) and 1.23 eV (Ref. 10) above the lowest exciton were accessed.

These observations are consistent with multipulse transient absorption studies by Frolov *et al.*¹¹ These experiments were similar to the photocurrent cross-correlation measurements, but the evolution of the sequentially excited state was monitored optically with a femtosecond probe pulse. The authors demonstrate that even-parity states can be classified as those that mediate charge transfer (those 1.1 eV above the $1B_u$ state), and those that promptly convert internally to $1B_u$. Neither the low-lying $1B_u$ state, or the lowest optically active state that couples to it (mA_g), dissociate with measurable efficiency. This suggests that high-energy A_g states have a different electronic character than low-energy ones.

In this paper, we conclude that efficient exciton dissociation occurs after sequential excitation to a high-energy state

following ultrafast photoexcitation. The sequentially excited state accessed in this experiment is at approximately twice the energy of the $1B_u$ state, significantly higher than those accessed in previous measurements. The dissociation yield is found to be $\sim 11\%$ under such conditions, but about two orders of magnitude lower under CW excitation conditions, when excited at a photon energy resonant with the $\pi \rightarrow \pi^*$ gap. This provides important evidence that direct charge generation is not an efficient process in the polymer studied herein.

II. EXPERIMENTAL

The synthesis of PIFTO is described in detail elsewhere.¹² Films of ~ 100 -nm thickness were spun, in a nitrogen-filled glove box, from anhydrous *p*-xylene solutions prepared under a nitrogen atmosphere, and were at no time exposed to air. During all of the experiments reported herein, samples were kept either under a dynamic vacuum ($< 10^{-5}$ mbar) at room temperature, or under an inert atmosphere at low temperature, to avoid photo-oxidation of the polymer. Femtosecond laser pulses at a 1-kHz repetition rate were derived from a home-built, dye-amplified Ti:sapphire laser system described in detail elsewhere.¹³ The pump beam at 3.18 eV (390 nm) was focused on the sample to a ~ 125 μm spot. The weaker probe beam, consisting of a single-filament white-light continuum generated in a sapphire substrate, was focused to ~ 50 μm in the same region of the sample after passing through a computer-controlled variable optical delay. Both pump and probe beams were horizontally linearly polarized. Spectrally resolved measurements of the fractional change in probe transmission due to the pump pulse ($\Delta T/T$) were performed with a 0.25-m spectrometer and a Peltier-cooled CCD camera. The chirp across the white-light continuum was numerically corrected using an empirical determination of the dispersion. Alternatively, single probe-wavelength measurements were made by detecting a spectrally narrow portion of the dispersed probe beam with a pair of Si photodiodes measuring the probe light transmitted through the sample and a reference beam, and lockin techniques. Continuous-wave photoinduced absorption (CW-PIA) measurements were performed with the sample mounted in a helium flow cryostat fitted with a heating element and a temperature controller, as described elsewhere.¹⁴ The temperature was monitored separately with a calibrated Si diode located near the sample. Mechanically modulated UV lines of an argon-ion laser at 351 and 364 nm were simultaneously used as the excitation source. A monochromated 150-W halogen-tungsten lamp was the probe light source. A Si photodiode or a liquid nitrogen-cooled InSb photodiode provided detection of the probe light, depending on the wavelength range, after passing through a second monochromator. $\Delta T/T$ was measured as a function of wavelength using lockin techniques, with the phase set to maximize the polymer PL signal in the X (in-phase) channel. Photoinduced absorption due to long-lived excitations thus appeared as negative signals in the X channel, accompanied by a positive signal in the Y ($\pi/2$ out of phase) channel. The magnitude of the CW-PIA signal is $R = \sqrt{X^2 + Y^2}$. The PL

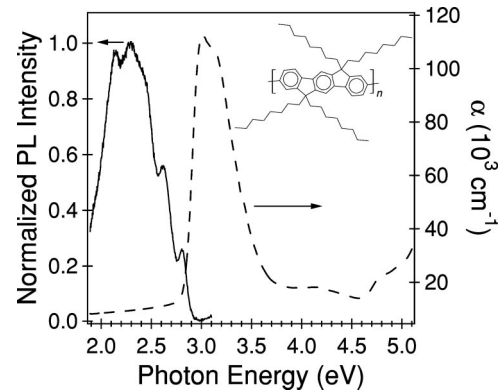


FIG. 1. Steady-state absorption (dashed line) and time-integrated photoluminescence (continuous line) spectra of PIFTO, with its structure included in the inset.

signal was subtracted by measuring it separately from the CW-PIA signal at each wavelength. Photovoltaic devices were prepared by spin coating from solution onto glass substrates coated with indium-tin-oxide (ITO). Prior to coating, the substrates were cleaned in an ultrasonic bath with acetone and *iso*-propanol, and subsequently treated in an oxygen-plasma. Aluminum contacts were deposited by thermal evaporation onto the polymer film. The diodes were electrically characterized under a dynamic vacuum of order 10^{-7} mbar. For determination of the spectral response of the photocurrent, a monochromated xenon arc lamp illuminated the diodes from the ITO side.

III. RESULTS AND DISCUSSION

The polymer used in this study is poly-6,6',12,12'-tetraoctyl-2,8-indenofluorene (PIFTO) (Ref. 12) which is a model blue-emitting conjugated polymer that we have shown to form relatively well ordered films compared to a similar material with branched 2-ethylhexyl side groups.¹⁵ The absorption and photoluminescence (PL) spectra of a PIFTO thin film are displayed in Fig. 1. The PL spectrum consists of blue emission from the conjugated backbone, superimposed with a broad, redshifted emission towards the green region of the spectrum, attributed to interchain species.¹⁵ Figure 2(a) shows the femtosecond transient absorption spectrum probed 1 ps (open circles) and 800 ps (dots) after photoexcitation of the $\pi \rightarrow \pi^*$ transition with a ~ 100 -fs optical pulse at moderately high pump fluence (~ 400 $\mu\text{J}/\text{cm}^2$). Figure 2(b) displays the time evolution of probe-induced stimulated emission (SE) of photoexcited chromophores, which probes exciton population density, at 2.64 eV (solid circles). The decay of the photoinduced absorption (PA) signal at 2.14 eV is also shown (open squares), which we have previously assigned to superimposed absorption of the lowest ($1B_u$) exciton and polaron pairs.¹⁵ The dynamics display picosecond and subpicosecond decay components characteristic of gain depletion by amplification of spontaneous emission (ASE) driven by wave guiding in the plane of the film,^{16,17} which leads to lasing in the presence of optical feedback in microcavity device architectures.¹⁸ Exciton bimolecular annihilation also increases the initial decay

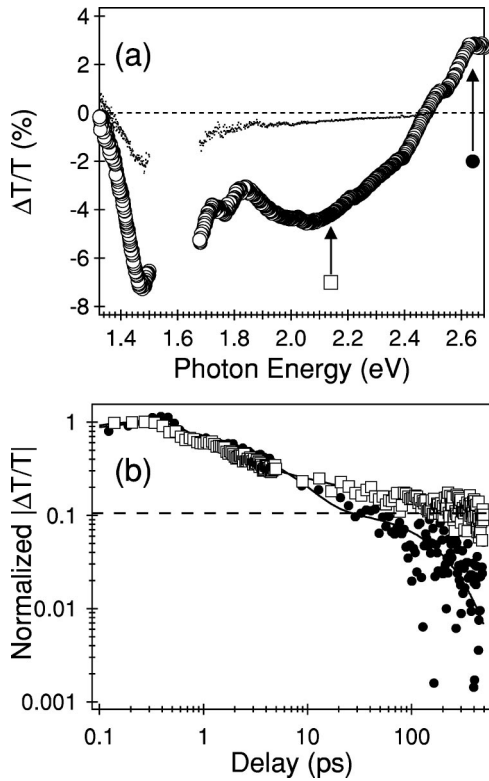


FIG. 2. (a) Pump-probe spectra probed 1 ps (open circles) and 800 ps (dots) after photoexcitation at 3.18 eV and $\sim 380 \mu\text{J}/\text{cm}^2$ fluence. Even at this pump fluence the initial $\Delta T/T$ did not degrade significantly over the time required to perform the measurement (~ 1 h). The sample was also translated to a fresh region periodically to avoid degradation effects. (b) Time decay of the normalized transient absorption signal at 2.64 eV (filled circles) and 2.14 eV (open squares) with similar excitation fluence as in (a). The dynamics at 1.46 and 2.64 eV are similar at this fluence range (see Ref. 13). The solid lines through the data are fits to $\sum A_i \exp(-t/\tau_i)$ convoluted with the instrument response function. The dashed line highlights the residual photoinduced absorption at 2.14 eV.

rate.⁸ A ~ 100 -ps excited state decay is observed. In addition, the PA data at 2.14 eV display a nanosecond decay components with $\sim 10\%$ total amplitude. Similar spectral features have been reported in a comprehensive study of phenylene-based conjugated polymers by Kraabel *et al.*¹⁹

We assign the long-lived PA component that is observed in the visible [Fig. 2(b)] to absorption of polaron pairs. Charged excitations in disordered conjugated polymers can be regarded as molecular radical ions.²⁰ Polaronic relaxation of the local electronic and lattice structure in the vicinity of charges shifts the energy levels with respect to those of the neutral polymer, inducing sub-gap optical transitions upon polaron formation. Figure 3(a) displays CW-PIA measurements on a PIFTO thin film at room temperature (continuous line) and at 20 K (dashed line), collected with a pump modulation frequency of 113 Hz. The room-temperature data are characterized by a broad feature centered at ~ 1.86 eV. In order to demonstrate that this peak is due to polaron pairs, semiconductor nanocrystal/conjugated polymer blends, which undergo photoinduced charge transfer¹⁴ and produce

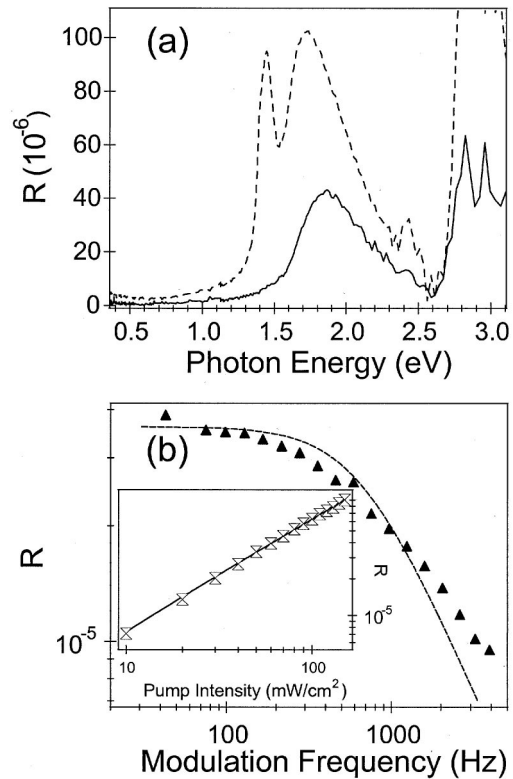


FIG. 3. Quasi-steady-state photoinduced absorption spectra at 298 K (continuous line) and 20 K (dashed line). Excitation was achieved with the 3.406 and 3.532 eV lines of an Ar^+ laser, modulated at 113 Hz, and with laser intensity of $38 \text{ mW}/\text{cm}^2$. (b) Pump frequency modulation dependence of the signal at 1.864 eV and at room temperature. The dashed line is a fit to a standard unimolecular decay expression $R \propto \tau / \sqrt{1 + \omega^2 \tau^2}$, with $\tau = 2.4 \times 10^{-4}$ s. Inset: room-temperature pump intensity dependence of the signal at a modulation frequency of 113 Hz. The solid line in the inset is a fit with $R \propto I^{0.9}$.

efficient photovoltaic devices,²¹ were also investigated. Room-temperature measurements on a 4.6-nm CdSe nanocrystal/PIFTO blend (25% nanocrystal by weight) exhibit 50% enhancement of this spectral feature (not shown here). Figure 3(b) shows the room-temperature modulation frequency dependence of the magnitude of the CW-PIA signal at 1.864 eV. The inset displays the room-temperature pump intensity dependence of the signal. The intensity dependence is essentially linear over all of the intensity range. For a monomolecular decay process, the signal is linear with intensity at all frequencies, it behaves as ω^{-1} for $\omega t \gg 1$, and it is independent of ω for $\omega t \ll 1$.²² We note that the spectra displayed in Fig. 3(a) are collected in a regime where the signal is independent on ω . We can conclude that the ultrafast photoinduced absorption feature at 2.14 eV is a combination of singlet exciton (by comparison of transients at 2.14 and 2.64 eV) and polaron-pair absorption [by comparison of Figs. 2(a) and 3(a)].

At low temperature, a sharp triplet-exciton absorption feature is also observed at 1.44 eV, with similar distribution of lifetimes as the polaron signal. Matching features have been observed in the structurally related ladder-type poly-

p-phenylene (LPPP) (Refs. 23,24) and polyfluorene²⁵ derivatives. Photoinduced absorption of triplet excitons is not measured in the room-temperature CW-PIA experiment, indicating that the steady-state population of this species produced by intersystem crossing is low. However, it is possible that an ultrafast triplet generation mechanism also operates at high pump intensity via high-energy excited states. The long-lived photoinduced absorption feature near 1.5 eV [Fig. 2(a)] could be due to triplet excitons, but we have insufficient evidence to assign this feature definitively. Ultrafast triplet generation has been proposed in the literature by singlet fission²³ and by nongeminate, spin-parallel electron-hole fusion.²⁶

Exciton bimolecular annihilation has been demonstrated to be an important source of charged excitations in conjugated polymers on timescales of a few picoseconds and at sufficiently high photon density.⁸ However, in our ultrafast measurements, polaron pairs are generated faster than the instrument response of our transient absorption apparatus (~ 150 fs), which is over an order of magnitude too fast to be accounted for by bimolecular annihilation and thus indicates an additional generation mechanism. Figure 4(a) shows the absolute initial ($t=0$) transient absorption signal at 2.64 eV (SE, solid circles) and 2.14 eV (PA, open squares) probe photon energies, versus pump fluence. The initial exciton density, interrogated by SE, varies linearly below $\sim 30 \mu\text{J}/\text{cm}^2$. Above this value it shows saturated intensity dependence. On the other hand, the initial signal at 2.14 eV, assigned to a combination of polaron-pair and exciton absorption, displays much higher saturation fluence. The extra initial signal at 2.14 eV must originate from polaron pairs. Our observation of ultrafast exciton dissociation is in agreement with that of Moses *et al.*⁶

Linear intensity dependence can arise from sequential excitation to a higher electronic state during the femtosecond pump pulse, where the leading edge of the pulse generates excitons and the trailing edge excites the same excitons (during ultrafast adiabatic relaxation) to higher states. This situation arises for a saturated ground-state electronic transition and an unsaturated excited-state transition. In this regime the linear intensity dependence of the excited-state transition governs the overall intensity dependence. From the evidence of Fig. 4(a), we propose that sequential electronic excitation and subsequent charge separation is the principal source of polaron pairs on ultrafast time scales and at high pump fluence. If polaron pairs were generated directly,⁶ then we would expect these to have the same intensity dependence as excitons. We note that in previous work on conjugated oligomers, Klimov *et al.* have concluded that two-exciton states (biexcitons) are generated at high photoexcitation fluence.²⁷ In solid films, this species was believed to undergo charge transfer to produce polaron pairs. Recently, Wegewijs *et al.* demonstrated, using flash-photolysis time-resolved microwave conductivity methods, that upon sufficiently intense optical excitation, photoelectron emission is possible in conjugated polymers.²⁸ This was found to occur by two-step photoexcitation from the ground state.

We implement a kinetic model [see inset of Fig. 4(b)] to explore this mechanism. The exciton (n_{ex}) and polaron-pair

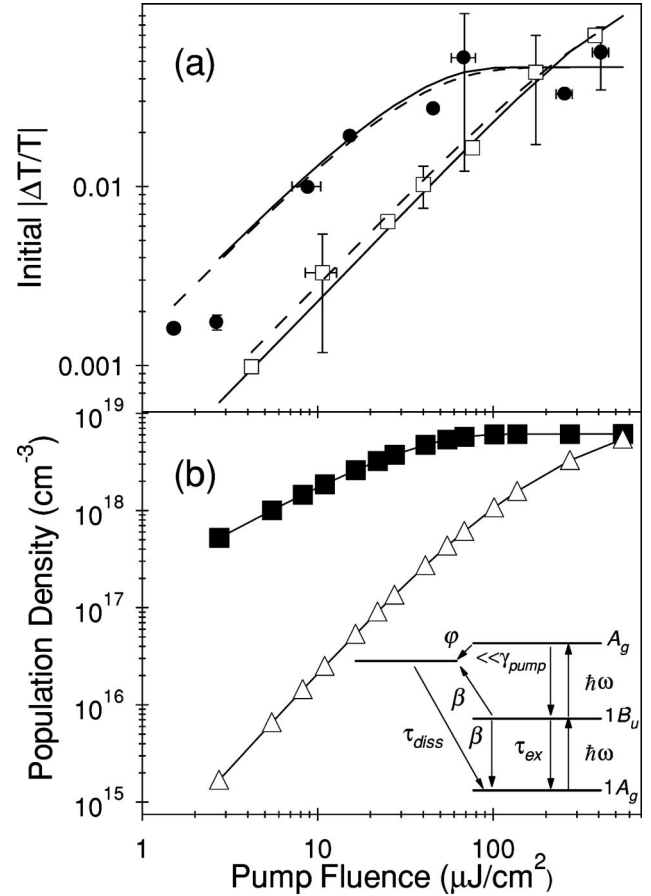


FIG. 4. Dependence on the photoinduced exciton and polaron-pair populations on the femtosecond pulse fluence. (a) Initial absolute transient absorption signal at 2.64 eV (filled circles) and 2.14 eV (open squares) photon energies, determined from the $t=0$ value of multiexponential fits to the data (see the caption of Fig. 2). The saturation fluence for the initial signal at each probe photon energy was determined from fits (shown as dashed lines) to a photodepletion expression of the form $[1 - \exp(-\Phi/\Phi_{\text{sat}})]$, where Φ is the pump pulse fluence. The saturation fluence was $\Phi_{\text{sat}} = 31.9$ and $411 \mu\text{J}/\text{cm}^2$ at 2.64 and 2.14 eV probe photon energies, respectively. The solid lines are results from the photophysical model. (b) Results from the photophysical model describing prompt charge generation by sequential excitation. Shown are the exciton (filled square) and polaron densities (triangles) at times $t \sim \gamma_{\text{pump}}$ (i.e., immediately after the photoexcitation pulse) at various pump fluences. The inset shows a schematic of the photophysical model.

(n_{diss}) population densities are given, respectively, by

$$\frac{dn_{\text{ex}}}{dt} = R(t)n_g - \frac{n_{\text{ex}}}{\tau_{\text{ex}}} - \beta n_{\text{ex}}^2 - G(t)n_{\text{ex}}, \quad (1)$$

$$\frac{dn_{\text{diss}}}{dt} = G(t)n_{\text{ex}} + \frac{\beta}{2}n_{\text{ex}}^2 - \frac{n_{\text{diss}}}{\tau_{\text{diss}}}, \quad (2)$$

where n_g is the ground-state chromophore density, τ_{ex} and τ_{diss} are the exciton and polaron-pair unimolecular time decay constants, respectively, and β is the diffusion-limited exciton bimolecular annihilation rate constant. We have demonstrated that in this class of blue-emitting materials, a

TABLE I. Summary of parameters used in the kinetic model.

| Parameter | Value |
|---|--|
| n_i | $7.94 \times 10^{18} \text{ cm}^{-3}$ |
| $\alpha_g (\hbar \omega_{\text{pump}} = 3.18 \text{ eV})$ | $1.012 \times 10^5 \text{ cm}^{-1}$ |
| β | $2.8 \times 10^{-8} \text{ cm}^2 \text{ s}^{-1}$ |
| τ_{ex} | 100 ps |
| τ_{ch} | 1000 ps |
| φ | 0.1 |

^aMeasured in Ref. 15

diffusion-limited mechanism dominates bimolecular annihilation.¹³ The fraction of exciton dissociation by this mechanism has been reported to be as high as 0.5 for PPV,⁸ and this accounts for the factor of 1/2 in the bimolecular annihilation term in Eq. (2). However, we have found that in a polyfluorene derivative, the fraction of exciton dissociation by bimolecular annihilation is significantly lower than this figure.¹³ The time scale for exciton dissociation by bimolecular annihilation is roughly an order of magnitude slower than that by sequential excitation during the pump pulse, so the polaron-pair density at $t=0$ is not affected by this term. The true yield of polaron pairs by bimolecular annihilation is not the focus of this work.

The rate constant of ground-state pumping by the femtosecond pulse $R(t)$ is given by

$$R(t) = \frac{\sigma_g f_{\text{pump}}}{\sqrt{2\pi} \gamma_{\text{pump}}} \exp\left[-\frac{t^2}{2\gamma_{\text{pump}}^2}\right], \quad (3)$$

where σ_g is the ground-state absorption cross section in cm^2 , f_{pump} is the pump photon flux in photons/ cm^2 , and γ_{pump} is related to the pump pulsewidth. The exciton dissociation rate constant $G(t)$ is given by

$$G(t) = \varphi \cdot R(t), \quad (4)$$

where φ is the composite polaron-pair yield, effectively the product of the excited-state-to-ground-state absorption cross-section ratio and the dissociation yield. Note that amplification of spontaneous emission (ASE) (Refs. 16,17) is not taken into account in this model. Neglect of this process leads to a slight overestimate of the early-time ($1B_u$) population. However, related measurements on other blue-emitting step-ladder conjugated polymer samples, with film thickness below the cutoff for ASE, indicate that this effect is not significant and that exclusion of ASE effects does not limit the conclusions presented herein. The related results are presented elsewhere.¹⁵

Time-dependent exciton and polaron-pair population densities were numerically calculated by solving equations 1 and 2 with a Runge-Kutta algorithm. Physically realistic input parameters were used in the simulation, and are reported in Table I. The initial ground-state chromophore density n_i was chosen so that the ground-state absorption cross section led to the correct experimental initial SE saturation fluence (see Fig. 4) given the ground-state absorption coefficient α_g . This was done via²⁹

$$\alpha_g = \sigma_g [n_i - n_{\text{ex}}] \approx \sigma_g n_i \quad (5)$$

which holds as long as the measurement of α_g is made far from saturation. The bimolecular annihilation rate constant was deduced from intensity-dependent, time-integrated PL measurements, which were reported earlier.¹⁵

Figure 4(b) plots early time ($t \sim \gamma_{\text{pump}}$) n_{ex} (solid squares) and n_{diss} (open triangles) as a function of pump fluence from the kinetic model. When the initial exciton density is saturated, the initial polaron-pair density varies linearly with pump fluence because the excited-state transition is not yet saturated. To match the kinetic modeling to the experimental results [Fig. 4(a)] requires one adjustable parameter. Importantly, this is the composite polaron-pair yield φ and the fitted data is for $\varphi=0.1$. The solid curve is simply the normalized initial exciton density shown in Fig. 4(b), while the dashed curve is a combination of exciton and polaron-pair densities. We note that significantly smaller yields (such as those measured under CW excitation conditions—see below) do not reproduce the results successfully.

It is important to estimate the yield of photoinduced polaron pairs. In the ultrafast experiment, multiexponential fits to the data at a pump fluence of $380 \mu\text{J}/\text{cm}^2$, displayed in Fig. 2(a) give $\sim 10\%$ of the total initial signal amplitude to the slowest decay component, assigned to polaron-pair absorption. The population density is related to $\Delta T/T$ via

$$n_{\text{diss}} = \frac{-1}{\sigma_{\text{diss}} z} \ln\left(\frac{\Delta T}{T} + 1\right), \quad (6)$$

where z is the thickness of the film. From the measured signal at $t=0$ shown in Fig. 4(a), the initial polaron-pair density is then $7 \times 10^{18} \text{ cm}^{-3}$, in reasonable agreement with the densities calculated from the photophysical model [Fig. 4(b)], assuming an absorption cross section of $\sim 10^{16} \text{ cm}^2$. This value was reported for LPPP, which is closely related to the material reported here.³⁰ The initial polaron-pair photo-generation yield (number of these per incident photon) is then $\sim 11\%$ at this pump fluence, consistent with that reported by Moses *et al.*⁵ In the CW experiment [Fig. 3(a)], the photoinduced charge density is estimated to be $4 \times 10^{16} \text{ cm}^{-3}$ at room temperature from the peak signal level (which is appropriate since the CW-PIA signal is independent on modulation frequency in that regime) and assuming the absorption cross section as above. From the time-integrated incident photon densities, the estimated charge generation yield is $< 0.1\%$. This measured yield is consistent with that reported by Wohlgenannt *et al.*²³ Note that the peak intensity of the femtosecond pulses at the highest fluence is a few GW/cm^2 , compared with the maximum intensity of $\sim 100 \text{ mW}/\text{cm}^2$ in the CW experiment. We have undertaken steady-state photocurrent measurements in a PIFTO photodiode with CW excitation (see Fig. 5). The peak external quantum efficiency (EQE) is only 0.028%, consistent with the optical yield measured in CW-PIA measurements. Separate photocurrent measurements in photodiodes based on polymer blends that exhibit photoinduced charge transfer reveal that the EQE increases from similarly small values in the homopolymer by over three orders of magnitude in the

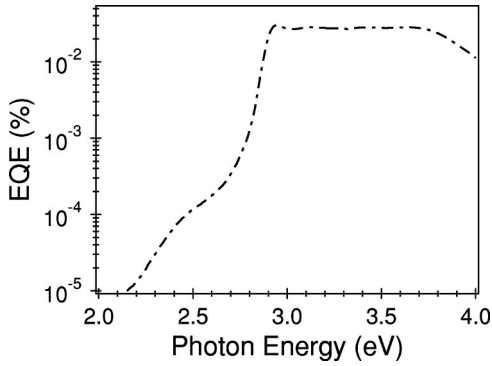


FIG. 5. Short-circuit photocurrent action spectrum of a PIFTO photovoltaic device. Shown is the spectral dependence of the external quantum efficiency (EQE), defined as the number of carriers collected per incident photon. The action spectrum has been corrected for the absorption spectrum of the ITO-coated glass substrate. It follows the absorption spectrum of the polymer.

blend.³¹ However, the photoluminescence quantum yield is only quenched by an order of magnitude. Care must be taken when comparing photocurrent data with the CW-PIA data, since the contact potentials of the electrodes provide a built-in electric field which could facilitate dissociation of weakly-bound polaron pairs, and may overestimate the exciton dissociation yield. However, we conclude that the photo-carrier yield in pristine conjugated polymers under “normal” excitation conditions is low, indicating that polarons are not direct photoexcitations in conjugated polymers.

While the observation of efficient exciton dissociation in ultrafast timescales is in agreement with Moses *et al.*,⁶ the conclusion concerning the mechanism is not. In that report, the authors invoke direct charge photogeneration. However, we cannot arrive at the same conclusion from the pump fluence dependence data shown in Fig. 4(a). If direct generation of polaron pairs were to occur in our material, then we would expect a saturated polaron-pair density in a regime where the ground-state transition is saturated. This is clearly not the case and we must therefore conclude that two-step excitation is the mechanism for exciton dissociation.

Note that in this work we refer to the ultrafast dissociation species as polaron pairs as opposed to free polarons (which are responsible for the photocurrent in a diode and the CW-PIA signal of a semiconductor nanocrystal blend, described above). The absorption spectra of weakly bound polaron pairs and free polarons has been found to be similar in semiconductor conjugated polymers,^{32,33} rendering the assignment to one or the other species difficult to make. There is no evidence from our work at this stage concerning the branching ratio of free polarons versus weakly bound polaron pairs. The nanosecond decay components of the residual PA signal in the visible indicates that some geminate recombination occurs in this time scale, but the mechanism of dissociation of polaron pairs is beyond the scope of this report. The precise nature of the dissociation product is thus not of direct relevance to the conclusions reached herein.

The estimated yield of exciton dissociation in the ultrafast measurement is roughly an order of magnitude larger than

that measured by Köhler *et al.* in steady-state photocurrent measurements with high excitation photon energy.⁴ As has already been mentioned above, care must be taken when comparing ultrafast optical and steady-state photocurrent measurements because of built-in potentials in the diode structure and geminate recombination dynamics. Nevertheless, it is interesting to speculate on the effect of symmetry on the exciton dissociation yield. Access to high-energy states from the even-parity $1A_g$ ground state by one-photon absorption results in a final state has B_u symmetry. The initial states populated by resonant sequential transitions as reported herein involve the lowest-lying $1B_u$ excited state as an intermediate, and therefore have A_g symmetry. Efficient exciton dissociation may occur directly from such even-parity states,³⁴ as depicted in the inset of Fig. 4. Frolov *et al.* have demonstrated that in an alkoxy-substituted PPV derivative, mA_g states convert internally to $1B_u$, but kA_g states produce long-lived products with an efficiency that correlates with photocurrent efficiencies, indicating that this long-lived species are either polarons or precursor paired polarons.¹¹ Note that the kA_g state in that report has an onset at 1.1 eV, while the states that are accessed vertically in this report are approximately 3.2 eV above $1B_u$. Efficient exciton dissociation may also occur in of a lower-lying even parity state (kA_g) or an odd-parity state resulting from rapid internal conversion during ultrafast thermalization. CW-PIA measurements of a derivative of LPPP (Ref. 23) have been used to invoke an electron tunneling mechanism for dissociation of hot excitons prior to thermalization, at excitation photon energies above the $\pi \rightarrow \pi^*$ gap. Rothberg *et al.* investigated the correlation of the reduction of exciton population induced by stimulated emission with a femtosecond dump pulse, with the photocarrier population, by photocurrent cross-correlation signal.³⁵ In that study, the authors concluded that excitons only dissociate during thermalization (before a few picoseconds following photoexcitation). We do not have direct evidence to ascertain whether ultrafast photodissociation as reported herein is from an even-parity, high-energy state, or after rapid internal conversion and during thermalization. This issue is the subject of ongoing investigations in our group. However, it is clear from the work reported herein and from other femtosecond-resolved measurements^{9–11} that efficient dissociation of sufficiently high-energy states is considerably more efficient than of the optically active excitonic state.

IV. CONCLUSIONS

In conclusion, a combination of transient and quasi-steady-state photoinduced absorption studies were undertaken to measure the formation rate of charged excitations in a model conjugated polymer. In the ultrafast experiment at high pump fluence, polaron pairs are generated within the pumping process (i.e., < 150 fs) by sequential excitation from the electronic ground state to a higher excited state via the lowest exciton, followed by exciton dissociation. Under such conditions the polaron-pair yield is $\sim 10\%$. This extraordinarily large value is due to the comparatively high peak intensities accessible with femtosecond pulse excitation

and to the special properties of high-energy excitons that lead to efficient charge dissociation. These results have profound implications for the prospect of optically pumped lasers,³⁶ since in order to achieve sufficiently large excitation densities for lasing, a photon density regime in which effects discussed herein are important must be used. Resonant sequential excitation is a powerful method of preparing highly excited states with even parity, which will be exploited in the future as a tool to investigate the electronic structure of conjugated polymers. Particularly, questions that are posed by this work are whether it is general that even-parity states

dissociate promptly, and, how such states in conjugated polymers differ from molecules.

ACKNOWLEDGMENTS

This work was supported by the European Commission under Brite-Euram Contract No. BRPR-CT97-0469 ('OSCA') and by the EPSRC (Grant No. RG 25535). We thank David Ginger for providing CdSe nanocrystal solutions.

-
- ¹J.H. Burroughes, D.D.C. Bradley, A.R. Brown, R.N. Marks, K. Mackay, R.H. Friend, P.L. Burns, and A.B. Holmes, *Nature (London)* **347**, 539 (1990).
- ²R.H. Friend, R.W. Gymer, A.B. Holmes, J.H. Burroughes, R.N. Marks, C. Taliani, D.D.C. Bradley, D.A. dos Santos, J.L. Brédas, M. Lögdlund, and W.R. Salaneck, *Nature (London)* **397**, 121 (1999).
- ³J.H. Schön, C. Klok, A. Dodabalapur, and B. Batlogg, *Science* **289**, 599 (2000).
- ⁴A. Köhler, D.A. dos Santos, D. Beljonne, Z. Shuai, J.-L. Brédas, A.B. Holmes, A. Kraus, K. Müllen, and R.H. Friend, *Nature (London)* **392**, 903 (1998).
- ⁵D. Moses, A. Dogariu, and A.J. Heeger, *Chem. Phys. Lett.* **316**, 359 (2000).
- ⁶D. Moses, A. Dogariu, and A.J. Heeger, *Phys. Rev. B* **61**, 9373 (2000).
- ⁷B. Horowitz, *Solid State Commun.* **41**, 729 (1982).
- ⁸G.J. Denton, N. Tessler, M.A. Stevens, and R.H. Friend, *Synth. Met.* **102**, 1008 (1999).
- ⁹C. Zenz, G. Lanzani, G. Cerullo, W. Graupner, G. Leising, U. Scherf, and S. DeSilvestri, *Synth. Met.* **116**, 27 (2001).
- ¹⁰J.G. Müller, U. Scherf, and U. Lemmer, *Synth. Met.* **119**, 395 (2001).
- ¹¹S.V. Frolov, Z. Bao, M. Wohlgenannt, and Z.V. Vardeny, *Phys. Rev. Lett.* **85**, 2196 (2000).
- ¹²S. Setayesh, D. Marsitzky, and K. Müllen, *Macromolecules* **33**, 2016 (2000).
- ¹³M.A. Stevens, C. Silva, D.M. Russell, and R.H. Friend, *Phys. Rev. B* **63**, 165213 (2001).
- ¹⁴D.S. Ginger and N.C. Greenham, *Phys. Rev. B* **59**, 10 622 (1999).
- ¹⁵C. Silva, D.M. Russell, M.A. Stevens, J.D. MacKenzie, S. Setayesh, K. Müllen, and R.H. Friend, *Chem. Phys. Lett.* **319**, 494 (2000).
- ¹⁶F. Hide, M.A. Díaz García, B.J. Schwartz, M.R. Anderson, Q. Pei, and A.J. Heeger, *Science* **273**, 1822 (1996).
- ¹⁷G.J. Denton, N. Tessler, M.A. Stevens, and R.H. Friend, *Adv. Mater.* **9**, 547 (1997).
- ¹⁸N. Tessler, G.J. Denton, and R.H. Friend, *Nature (London)* **382**, 695 (1996).
- ¹⁹B. Kraabel, V.I. Klimov, R. Kohlman, S. Xu, H.L. Wang, and D.W. McBranch, *Phys. Rev. B* **61**, 8501 (2000).
- ²⁰M. Deussen and H. Bässler, *Synth. Met.* **54**, 49 (1993).
- ²¹W.U. Huynh, X. Peng, and A.P. Alivisatos, *Adv. Mater.* **11**, 923 (1999).
- ²²G. Dellapiane, C. Cuniberti, D. Comoretto, G.F. Musso, G. Figari, A. Piaggi, and A. Borghesi, *Phys. Rev. B* **48**, 7850 (1993).
- ²³M. Wohlgenannt, W. Graupner, G. Leising, and Z.V. Vardeny, *Phys. Rev. B* **60**, 5321 (1999).
- ²⁴M. Wohlgenannt, C.P. An, and Z.V. Vardeny, *J. Phys. Chem. B* **104**, 3846 (2000).
- ²⁵A.J. Cadby, P.A. Lane, H. Mellor, S.J. Martin, M. Grell, C. Giebeler, D.D.C. Bradley, M. Wohlgenannt, C. An, and Z.V. Vardeny, *Phys. Rev. B* **62**, 15 604 (2000).
- ²⁶C. Zenz, G. Cerullo, G. Lanzani, W. Graupner, F. Meghdadi, G. Leising, and S. De Silvestri, *Phys. Rev. B* **59**, 14 336 (2000).
- ²⁷V.I. Klimov, D.W. McBranch, N. Barashkov, and J. Ferraris, *Phys. Rev. B* **58**, 7654 (1998).
- ²⁸B.R. Wegewijs, G. Dicker, J. Piris, A.A. García, and J.M. Warman, *Chem. Phys. Lett.* **332**, 79 (2000).
- ²⁹W. Demtröder, *Laser Spectroscopy* (Springer, Berlin, 1996).
- ³⁰A. Haugender, M. Neges, C. Kallinger, W. Spirkel, U. Lemmer, J. Feldmann, U. Scherf, A. Gügel, and K. Müllen, *Phys. Rev. B* **59**, 15 346 (1999).
- ³¹A. C. Arias, J. D. MacKenzie, R. Stevenson, J. J. M. Halls, M. Inbasekran, E. P. Woo, D. Richards, and R. H. Friend, *Macromolecules* **34**, 6005 (2001).
- ³²E.M. Conwell and H.A. Mizes, *Synth. Met.* **78**, 201 (1996).
- ³³P.A. Lane, X. Wei, and Z.V. Vardeny, *Synth. Met.* **84**, 521 (1997).
- ³⁴A. Chakrabarti and S. Mazumdar, *Phys. Rev. B* **59**, 4839 (1999).
- ³⁵L.J. Rothberg, M. Yan, A.W.P. Fung, T.M. Jedju, E.W. Kwock, and M.E. Galvin, *Synth. Met.* **84**, 537 (1997).
- ³⁶F. Hide, M.A. Díaz García, B.J. Schwartz, and A.J. Heeger, *Acc. Chem. Res.* **30**, 430 (1997).